Received March 1999
Revised October 2000
Accepted October 2000

Coarse resolution large-eddy simulation of turbulent channel flows

J. Shi, T.G. Thomas and J.J.R. Williams
Department of Engineering, Queen Mary and Westfield College, London University, UK

Keywords *Eddy currents, Turbulence, Channels*

Abstract *In this paper two important factors – the subgrid model length scale and lateral resolution – are investigated for the large-eddy simulation (LES) of high Reynolds number turbulent channel flow using resolutions that are insufficient to fully resolve the buffer layer. It is found that the use of standard damping functions will not reproduce correct mean velocity profiles and that good LES results will only be obtained by adjustment of the subgrid model length scales. To also obtain accurate turbulence statistics then special attention has to be given to the lateral resolution.*

1. Introduction

In recent years, the use of LES for solving turbulent flows has gained popularity. The justification of LES approach comes from the fact that most problems of practical engineering interest are at high Reynolds numbers, however, even the most powerful computers available today are only feasible for direct simulation of turbulent flows at low or moderate Reynolds numbers. Therefore, for engineering problems with high Reynolds numbers, the large-eddy simulation is an important technique for simulation of turbulent flows. Previous research has revealed that the large scale turbulent eddies contain most of the energy, perform most of the turbulent transport, hence dominate the main properties of the turbulent flows. In LES, the temporal evolution of these dominating large scale eddies is explicitly and correctly resolved numerically and only the small scale eddies, which are more isotropic, random and have indirect influence to the large scale motions, are taken into account by a subgrid scale model (SGM).

Obviously, the success of the LES approach is affected by the performance of the subgrid model, i.e. how much kinetic energy from the resolved large-scale is dissipated by the SGM model. For decades there have been intensive efforts towards developing and investigating subgrid models. The most commonly accepted model today is the Smagorinsky model (Smagorinsky, 1963) which parameterizes an eddy viscosity. However, the formulation of the eddy viscosity involves an unknown subgrid length scale which has to be determined empirically. The Smagorinsky length scale, $L = C_s\Delta$, is a function of the mesh scale Δ and a value of a coefficient C_s. Germano *et al.* (1991), and more recently Ghosal *et al.* (1992; 1994) have developed a method to determine C_s dynamically during the simulation by measuring the energy transfer rates

International Journal of Numerical Methods for Heat & Fluid Flow, Vol. 11 No. 1, 2001, pp. 20-35.

close to the wavenumber cutoff. This is important in the simulation of inhomogeneous flows where C_s may vary with location. However, in homogeneous turbulent flows the variation of C_s is less important and reasonable results may be obtained with a fixed value of C_s for a given mesh scale. For channel flows, Deardorff (1970) suggested that $C_s = 0.1$ is the optimum magnitude.

It is well known that as the wall is approached the subgrid length scale has to be decreased in order to match Prandtl's mixing length function. Because most turbulent energy is generated in the near wall region, a matching function which links the Smagorinsky and Prandtl mixing length plays a key and sensitive role in a simulation since an incorrect matching function in the near wall and buffer regions will result in either damping out too much of the large-scale motions or producing excessive amounts of the subgrid-scale motions.

It is common knowledge that near the wall region a good vertical resolution is needed in order to capture the features of turbulent flow. In our study, however, we found that the lateral resolution is also very important for good results since the bursting phenomenon or streaky structure near the wall requires to be sufficiently resolved. A good coarse resolution LES result is determined, therefore, not only by a good subgrid model but also by resolving the low speed streaks.

In this paper we investigated the influence of the two factors: length scale and lateral resolution. Our study shows that for open channel flows at relatively high Reynolds number, the matching function using the standard van Driest damping factor (Thomas and Williams, 1995) will not give satisfactory results, whereas the Mason and Thomson's power matching function (Mason and Thomson, 1992) with correctly chosen powers can give reasonably good results for varying mesh scales as long as the lateral spacing scale y^+ is less than about 20. Also, the use of Schumann's (1975) split SGM with suitably chosen coefficients can also give correct mean velocity profiles.

The paper is organized as follows: section 2 briefly describes the governing equations and subgrid model used. Section 3 gives the numerical method and boundary conditions. Section 4 discusses the length scale and matching functions. Section 5 presents the numerical results and discussions. Section 6 is the conclusions.

2. Governing equations

The basic equations in large-eddy simulations are the usual volume averaged Navier-Stokes equations enhanced by an additional subgrid stress. For incompressible fluids they take the following form:

$$\frac{\partial u_i}{\partial x_i} = 0 \tag{1}$$

$$\frac{\partial u_i}{\partial t} + \frac{\partial (u_i u_j)}{\partial x_j} = -\frac{\partial p}{\partial x_i} + \frac{\partial \tau_{ij}}{\partial x_j} + g_i \tag{2}$$

where $(u_1, u_2, u_3) = (u, v, w)$ are the resolved velocity components in the $(x_1, x_2, x_3) = (x, y, z)$ representing streamwise, spanwise and vertical directions, respectively, p is the pressure, g_i is a source term and τ_{ij} is a stress tensor which is a combination of a normal viscous stress and a subgrid stress parametrized by a subgrid scale model (SGM). Although a free-surface code has been used for the simulations reported here the free-surface itself will have negligible effect on the results.

The time evolution of the elevation of the free surface, $h = f(x, y, t)$, is governed by a kinematic equation modeling the surface as it moves with the fluid. In vector form it gives:

$$\frac{\partial h}{\partial t} = (\underline{u} \cdot \underline{n})\sqrt{\sigma} \tag{3}$$

here $\underline{u} = (u, v, w)$ is the velocity vector,

$$\underline{n} = \left(-\frac{\partial h}{\partial x}, -\frac{\partial h}{\partial y}, 1\right)\frac{1}{\sqrt{\sigma}} \tag{4}$$

is the surface unit normal vector and

$$\sigma = 1 + \left(\frac{\partial h}{\partial x}\right)^2 + \left(\frac{\partial h}{\partial y}\right)^2 \tag{5}$$

3. Computational method

We consider the turbulent flow of an incompressible fluid flowing down an infinitely wide open channel. The free surface is allowed to deform arbitrarily and is subject only to a maximum slope limit (Thomas and Williams, 1994) such that

$$\left|\frac{\partial h}{\partial x}\right| \leq \frac{\Delta z}{\Delta x}, \left|\frac{\partial h}{\partial y}\right| \leq \frac{\Delta z}{\Delta y} \tag{6}$$

which allows a much simplified surface locator. The two characteristic lengths for this flow are the depth d and the viscous length ν/u_τ where u_τ denotes the characteristic shear velocity $(\alpha g d)^{1/2}$, α is the bed slope and g is the acceleration due to gravity. With u_τ and d set to unity we chose α to be equal $1/1,000$ and, consequently, g to be $1,000$. The ratio $u_\tau d/\nu$ is denoted Re^+ and is also set equal to $1,000$ whereas the ratio $u_s/\sqrt{gd}$ is the Froude number F_r in which u_s is the mean surface velocity and is determined by the simulation. With u_s approximately equal to 22.0 F_r becomes 0.7 and the Reynolds number based on the mean surface velocity $u_s d/\nu$ is approximately 22,000.

The time dependent incompressible Navier-Stokes equations with boundary conditions of a solid bed and a free surface are solved numerically until a statistically steady state has been reached. By averaging of the instantaneous flow field the mean flow field is obtained and, consequently, the fluctuating

values can be attained by subtracting the two fields. Finally, turbulent statistics can be calculated such as root-mean-square values (rms) and Reynolds-stresses.

3.1 Numerical discretization

The discrete form of the equations (1) and (2) used in our large-eddy simulations are obtained by a second-order central difference method applied to a staggered grid. The time advancement is by the second-order Adams-Bashforth method. If we denote the quantity

$$H_i^n = \left[-\frac{\delta u_i u_j}{\delta x_j} + \frac{\delta \tau_{ij}}{\delta x_j} + g_i \right]^n \qquad i, j \in [1,2,3] \tag{7}$$

$$G^n = -\left[\frac{\delta}{\delta x_1} \int_0^h u_1 dx_3 + \frac{\delta}{\delta x_2} \int_0^h u_2 dx_3 \right]^n \tag{8}$$

where n is the discrete time level and δ is the finite difference operator, the solution is advanced over a time step using the equations

$$\frac{\bar{u}_i - u_i^n}{\Delta t} = \frac{3}{2} H_i^n - \frac{1}{2} H_i^{n-1} + \frac{1}{2} \frac{\delta p^{n-1}}{\delta x_i} \tag{9}$$

$$\frac{u_i^{n+1} - \bar{u}_i}{\Delta t} = -\frac{3}{2} \frac{\delta p^n}{\delta x_i} \tag{10}$$

$$D^2 p^n = \frac{2}{3\Delta t} \frac{\delta \bar{u}_j}{\delta x_j} \tag{11}$$

$$\frac{h^{n+1} - h^n}{\Delta t} = \frac{1}{2} \left(G^{n+1} + G^n \right) \tag{12}$$

where $\bar{u}_i$ is an intermediate resolved velocity, Δt the time step, and D^2 the discrete Laplace operator.

Note that the continuity equation (1) is replaced by the Poisson equation (11). In this approach, first $\bar{u}_i$ is computed using (9), and continuity at time level $n+1$ is enforced by solving the Poisson equation (11) for the pressure, then the u_i^{n+1} velocity is computed by solving equation (10), finally the new surface elevation h^{n+1} is updated by implicit iteration of equation (12).

3.2 Subgrid model

In the present study we use the Smagorinsky model which is the most commonly used SGM. The stress tensor τ_{ij} is then defined as

$$\tau_{ij} = 2(\nu + \nu_s) S_{ij} \tag{13}$$

where ν denotes the kinematic viscosity and ν_s is the eddy viscosity, given by

$$\nu_s = L^2(2S_{ij}S_{ij})^{\frac{1}{2}} \tag{14}$$

and

$$S_{ij} = \frac{1}{2}\left(\frac{\partial u_i}{\partial x_j} + \frac{\partial u_j}{\partial x_i}\right) \tag{15}$$

where L is the length scale which will be discussed in section 4.

3.3 Boundary conditions

In this study periodic boundary conditions are used in the streamwise and lateral directions and a Schumann boundary condition (Schumann, 1975) is applied on the bed of the channel for the stress boundary condition. The Schumann boundary condition assumes that the instantaneous wall shear stress τ varies in phase with the instantaneous velocity components tangential to the bed such that $\tau = u < \tau > / < u >$ for the streamwise direction, likewise the spanwise direction. The $< \cdot >$ denotes the averaged value. The ratio between $< \tau >$ and $< u >$ can be determined from the law-of-the-wall which is the universally accepted velocity profile.

On the surface of the flow, the external boundary conditions imposed are zero pressure and tangential shear stress. The surface is freely deformable. The method of dealing with these is described in Thomas and Williams (1994) and Thomas *et al.* (1995) and their adopted procedures enable the free surface and any wave motion to be modelled accurately.

The previous discretized equations with the boundary conditions described above are solved by a LES code (Thomas *et al.*, 1995; Thomas and Williams, 1995) developed at Queen Mary and Westfield College, London University. This code can, therefore, be used to simulate turbulent open channel flows with freely deformable surface.

4. Problem definition

As discussed in section 3.2 the subgrid model involves a length scale L. Near the wall the small eddies are represented by a Prandtl mixing length $L = C_0 z^+$, where C_0 is von Karman's constant, z^+ is the distance to the bed which is normalized by the length ν/u_τ and is denoted by a superscript +. In the outer flow region the subgrid scale L is given by Deardorff (1970) and has the form $L = C_s\Delta$ where $\Delta = (\Delta x^+ \Delta y^+ \Delta z^+)^{\frac{1}{3}}$ and C_s is the Smagorinsky constant. To match the near-wall Prandtl mixing length to the length scale in the outer region, a matching function is required.

In our first test run the standard van Driest damping factor (Van Driest, 1956) which has the following expression:

$$\Gamma(z^+) = 1 - exp(-z^+/A) \tag{16}$$

was used, thus the length scale used in the first run is

$$L = C_s \Delta \Gamma(z^+) \tag{17}$$

where $A = 26$ is the van Driest constant.

For engineering interest we carried out our simulations at a Reynolds number $R_e^+ = 1,000$. The first run of our simulation begins with a box size of $6 \times 4 \times 1$ in streamwise, spanwise and vertical directions, respectively, and $C_s = 0.1$ was chosen. Two resolutions, 32^3 and 64^3 grids, were conducted.

Figures 1 and 2 show the comparison of the computed streamwise mean velocity normalized by the wall shear velocity and the experimental LDA data of Nezu and Rodi (1994) (hereafter denoted: NR). The solid line represents the law of the wall profile. In the viscous sublayer ($z^+ < 5$), the law of the wall follows a linear distribution $U^+ = z^+$. In the outer region ($z^+ > 30$), it follows $U^+ = 2.43lnz^+ + 5.29$.

From Figures 1 and 2 one can see that the van Driest damping function cannot give satisfactory results in that the computed profiles (box line) are much lower than the experimental data.

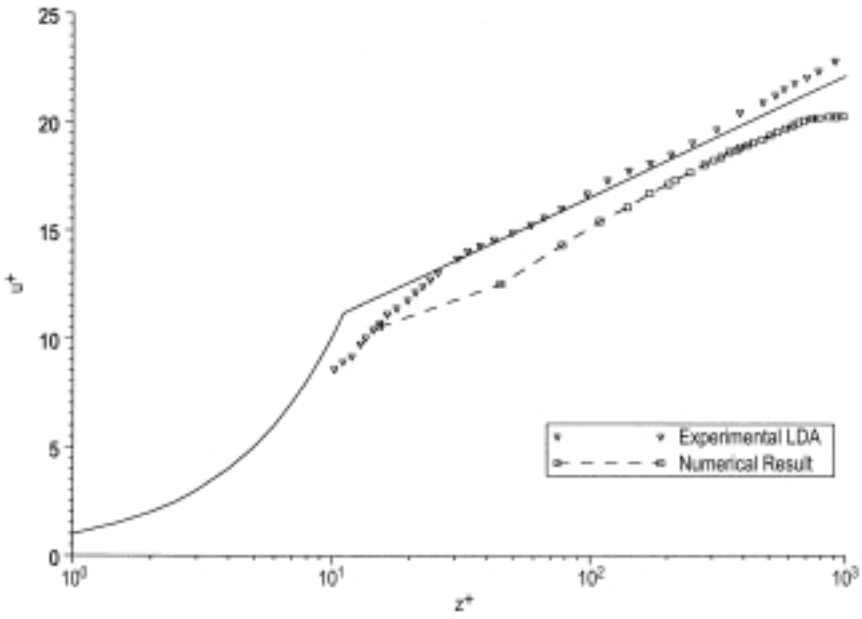

Figure 1.
Comparison of mean velocity in streamwise direction between computational solution and experimental result for box size $6 \times 4 \times 1$ with $32 \times 32 \times 32$ grid using van Driest damping factor

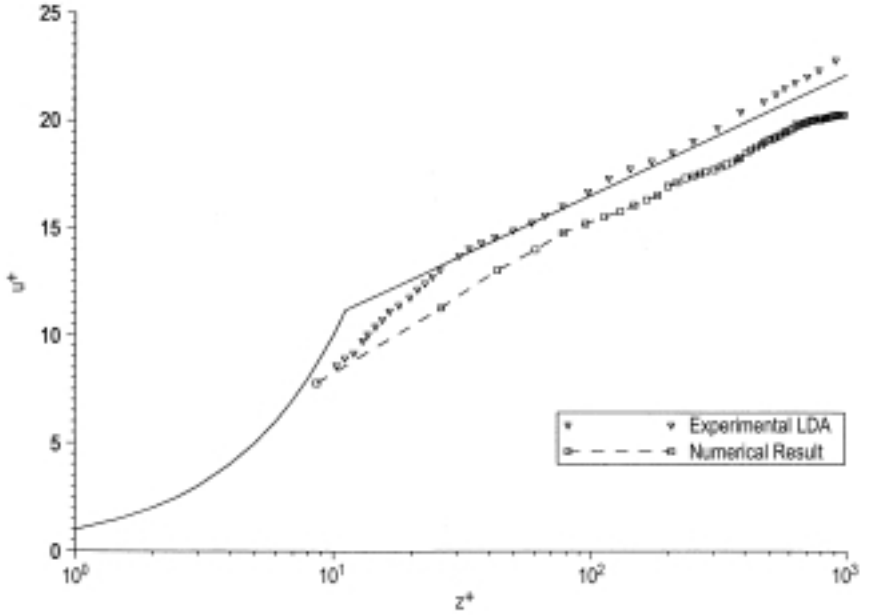

Figure 2.
Comparison of mean velocity in streamwise direction between computaional solution and experimental result for box size $6 \times 4 \times 1$ with $64 \times 64 \times 64$ grid using van Driest damping factor

5. Length scale and matching functions

In order to see how a length scale matching function affects the numerical results a function similar to that introduced by Mason and Thomson (1992) is used:

$$\frac{1}{L^n} = \frac{1}{L_1^n} + \frac{1}{L_2^n} \tag{18}$$

where:

$$L_1 = C_0 z^+ \Gamma(z^+) \tag{19}$$

$$L_2 = C_s \Delta \tag{20}$$

and $C_0 = 0.42$ is the von Karman constant.

Figures 3 and 4 show, for the 32^3 and 64^3 grids respectively, equation (18) for various values of n. It can be seen from these figures that as n increases, the sharper the profile becomes and approaches the Deardorff length scale L_2 (20) at much smaller values of z^+. The van Driest damping function is equivalent to Mason matching function with power between 1 and 2.

Figures 5 and 6 show the results which repeat the previous tests (see section 4) using matching function (18). For 32^3 grid case the power $n = 1$ and for 64^3 grid case the power $n = 0.5$ (see Figure 4) were used. In Figures 5 and 6 better agreement between the computed solution and the experiment data can be observed. From these results it can be seen that the length scale required for a suitable simulation is much less than that obtained by the use of either the standard van Driest damping function or Mason's damping function with the

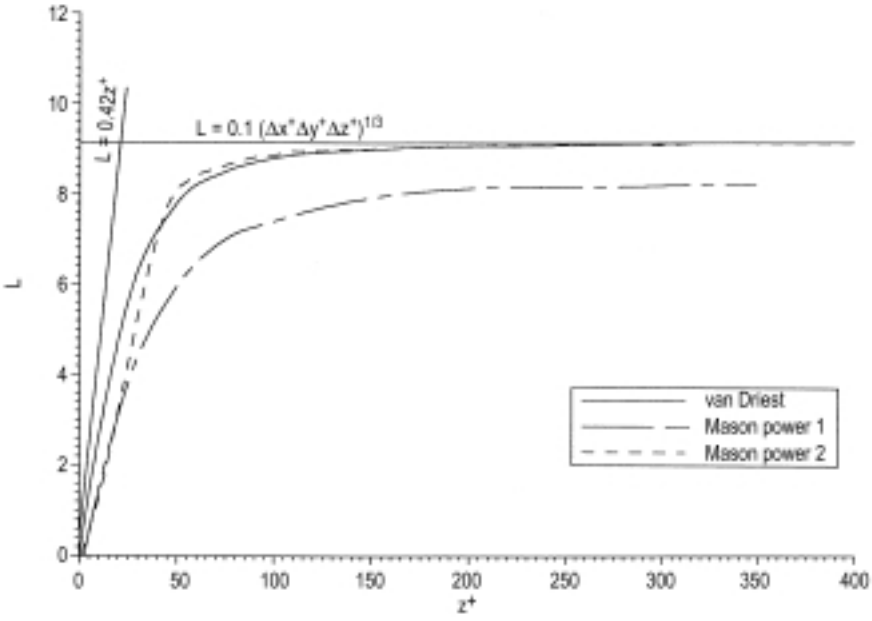

Figure 3.
Length scales for 32^3 grid

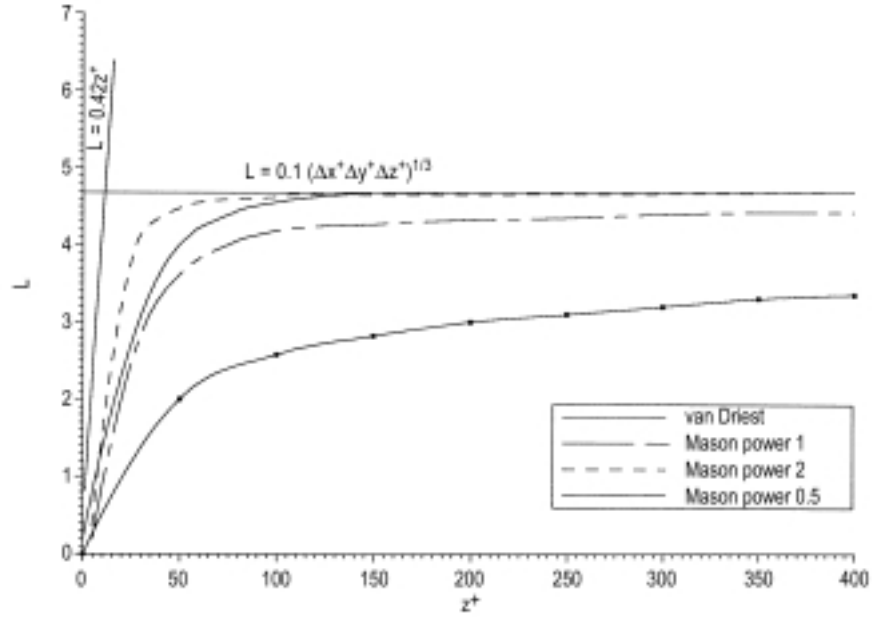

Figure 4.
Length scales for 64^3 grid

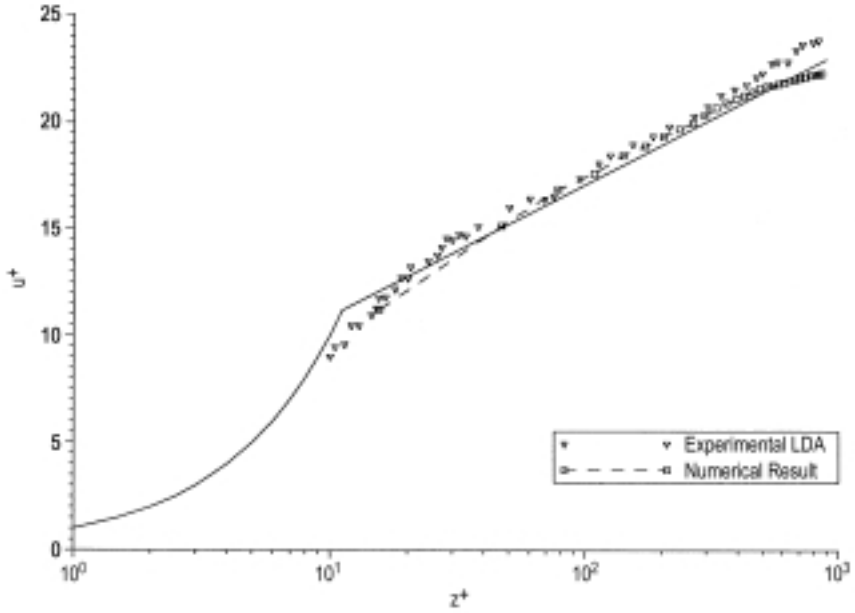

Figure 5.
Comparison of mean velocity in streamwise direction between computational solution and experimental result for box size $6 \times 4 \times 1$ with $32 \times 32 \times 32$ grid using Mason's function with power 1

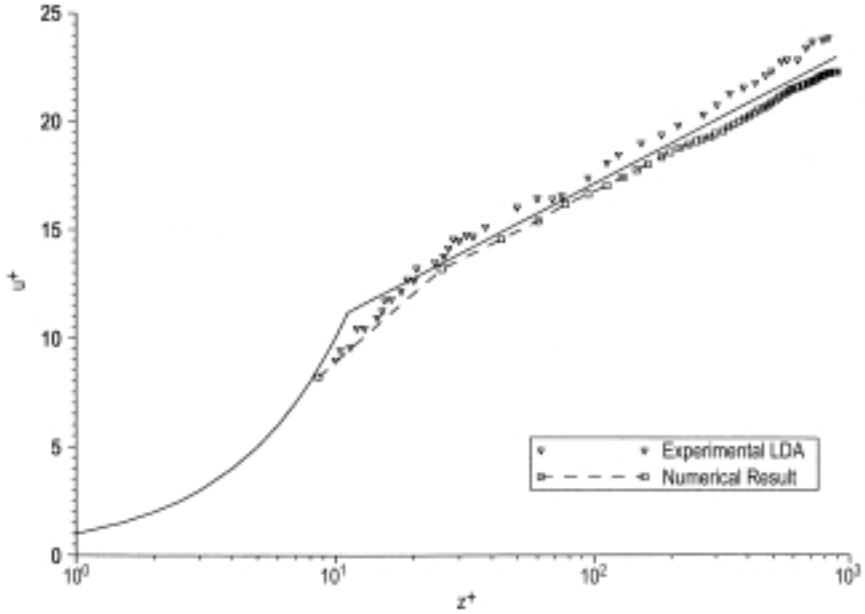

Figure 6.
Comparison of mean velocity in streamwise direction between computational solution and experimental result for box size $6 \times 4 \times 1$ with $64 \times 64 \times 64$ grid using Mason's function with power 0.5

recommended value of $n = 2$. These results are consistent with the findings of Moin *et al.* (1991) who indicated that values for C_s should lie between 0.06 and 0.08 and who carried out tests of direct numerical simulation (DNS) data of homogeneous shear flow.

6. Lateral resolution

Figures 7 and 8 show the computed turbulent rms values normalized by u_τ for the streamwise, spanwise and vertical directions compared to the experimental results. These are shown for the two grids (32^3 and 64^3) used in the last section. It can be seen that the vertical rms agree reasonably well with the measured data. However, large differences are evident between the numerical and measured streamwise and lateral rms values.

The lateral resolution for the 32^3 and 64^3 grids give Δy^+'s of 125 and 62.5 respectively. Both of these are considered to be too coarse to resolve the streaky structure near the bed wall and might be the cause of the low computed rms values. In order to test the effect of lateral resolution and to resolve the streaky structure near the bed wall better, we reduced the box size to $6 \times 0.5 \times 1$ with 32^3 grid, thus making the lateral spacing size $\Delta y^+ = 15.6$. Figures 9 and 10 show the comparison of the results and it can be seen that very good results were obtained. However, we have to point out that with this box size the flow in the upper part of the channel is highly correlated although we do not expect the results in the lower part to be affected. With this better resolution we are more able to resolve low speed streaks near the bed and excellent mean and turbulent results are produced although the box may be too narrow for outer region comparison.

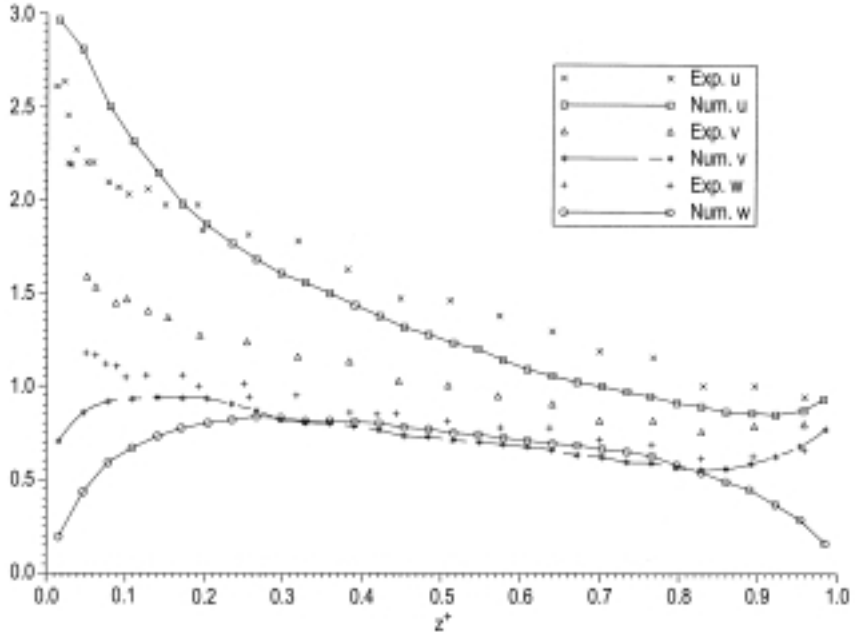

Figure 7.
Comparison of rms between computational solutions and experimental results for box size $6 \times 4 \times 1$ with $32 \times 32 \times 32$ grid using Mason's function power 1

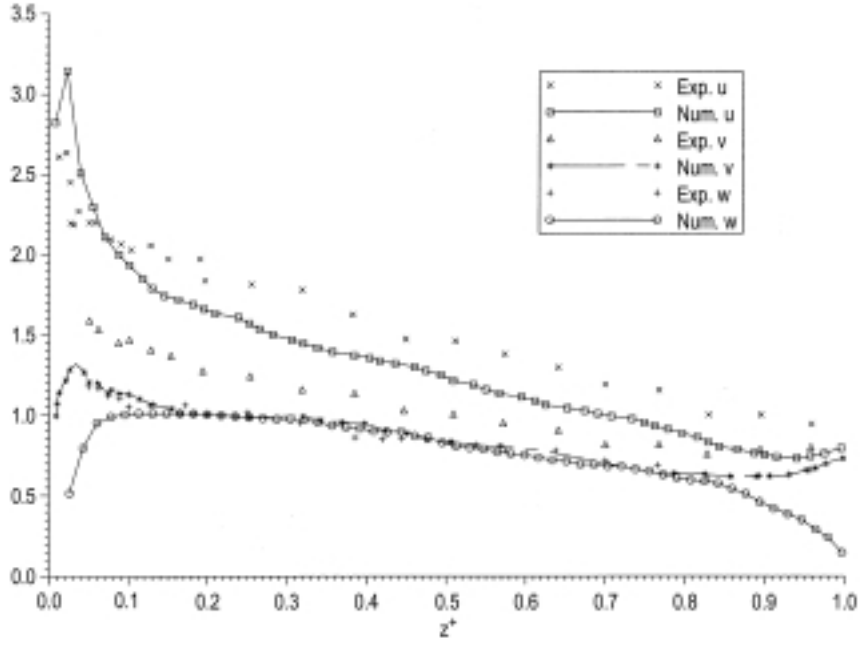

Figure 8.
Comparison of rms between computational solutions and experimental results for box size $6 \times 4 \times 1$ with $64 \times 64 \times 64$ grid using Mason's function power 0.5

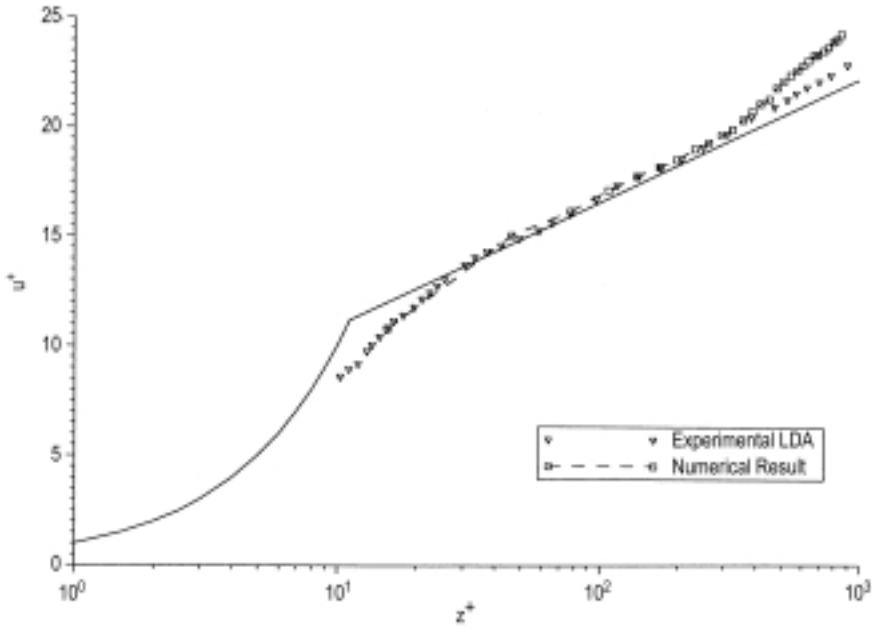

Figure 9.
Comparison of mean velocity in streamwise direction between computational solution and experimental result for box size $6 \times 0.5 \times 1$ with $32 \times 32 \times 32$ grid using Mason's function with power 1

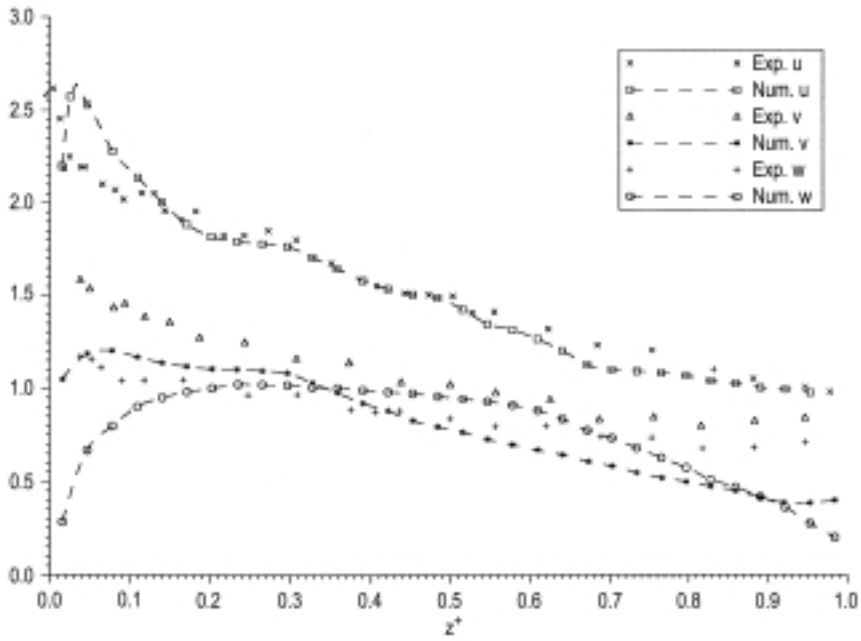

Figure 10. Comparison of rms between computational solutions and experimental results for box size $6 \times 0.5 \times 1$ with $32 \times 32 \times 32$ grid using Mason's function power 1

7. Split subgrid model

Simulations were also carried out using Schumann's (1975) split SGM:

$$\tau_{ij} = -2\nu_T(S_{ij} - < S_{ij} >) - 2\nu_T^* < S_{ij} > \tag{21}$$

where ν_T is the homogenous contribution to the eddy viscosity defined as:

$$\nu_T = (C\Gamma\triangle)^2[2(S_{ij} - < S_{ij} >)(S_{ij} - < S_{ij} >)]^{\frac{1}{2}} \tag{22}$$

and the anisotropic contribution is defined according to Moin and Kim (1982) as:

$$\nu_T^* = C^*(\Gamma^*\triangle_y)^2(2 < S_{ij} >< S_{ij} >)^{\frac{1}{2}}. \tag{23}$$

Here $\triangle_y$ is the filter width in the spanwise direction and $\Gamma^*(z^+) = 1 - exp[-(z^+/A)^2]$ with $A = 25$. To both ν_T and ν_T^* is added ν.

Figures 11 and 12 show a comparison of the computed streamwise mean velocity (normalized by u_τ) and the experimental NR data for the 32^3 and 64^3 grids respectively. It was found that in order to obtain correct mean velocity profiles C was set to 0.14 and 0.17 for the 32^3 and 64^3 grids respectively although other combinations may give equally good results. C^* was set to 0.013 for both grids. Thus indicating that the mean shear component in the standard Smagorinsky model can have a significant damping effect when relatively course grids are used. Also, a correct mean velocity profile could only be obtained for the 32^3 grid by ensuring that the first velocity point fell onto the

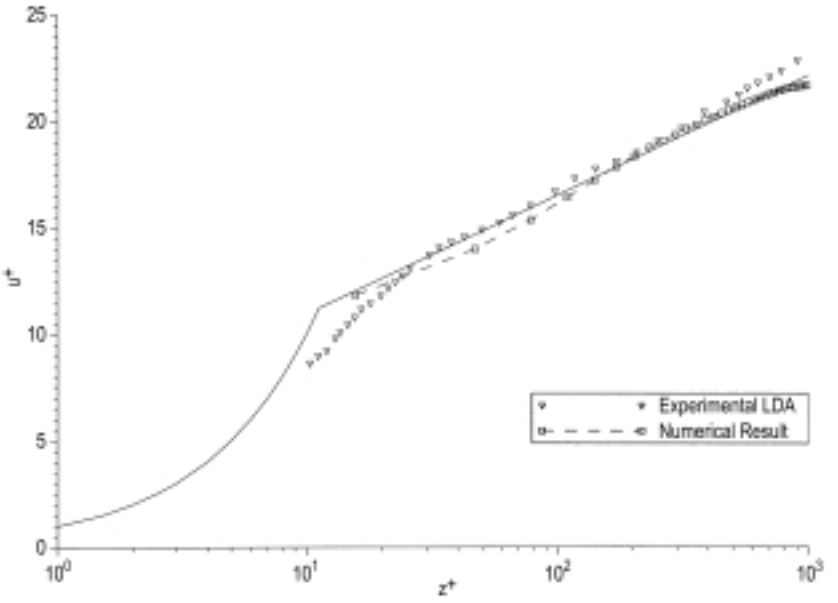

Figure 11.
Comparison of mean velocity in streamwise direction between computational solution and experimental result for box size $6 \times 4 \times 1$ with $32 \times 32 \times 32$ grid using Schumann's split SGM

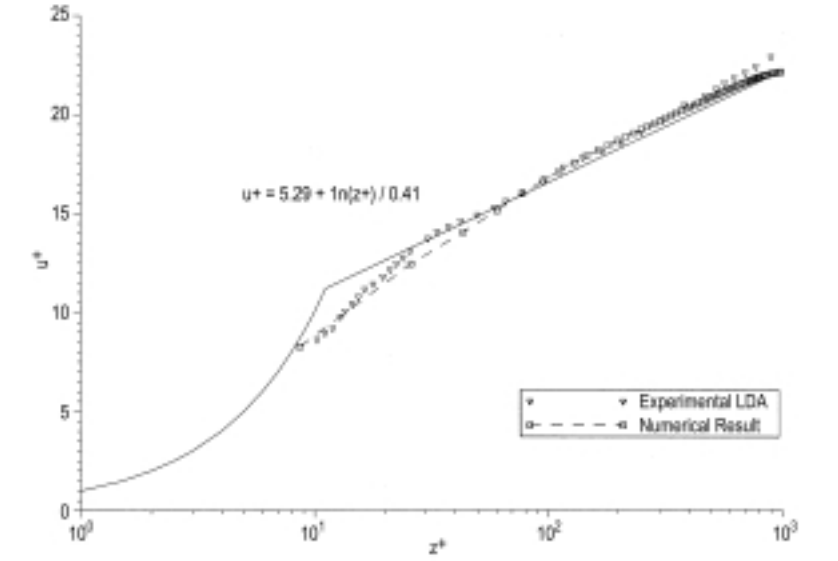

Figure 12.
Comparison of mean velocity in streamwise direction between computational solution and experimental result for box size $6 \times 4 \times 1$ with $64 \times 64 \times 64$ grid using Schumann's split SGM

log-law rather than onto its buffer region value. This was due to the fact that alteration of the coefficients was not able to produce a log-law line with a sufficiently large enough constant of integration – i.e. the correct slope was produced but the line always fell significantly below its correct value.

Figures 13 and 14 show the computed turbulent rms values normalized by u_τ for the streamwise, spanwise and vertical directions compared to the

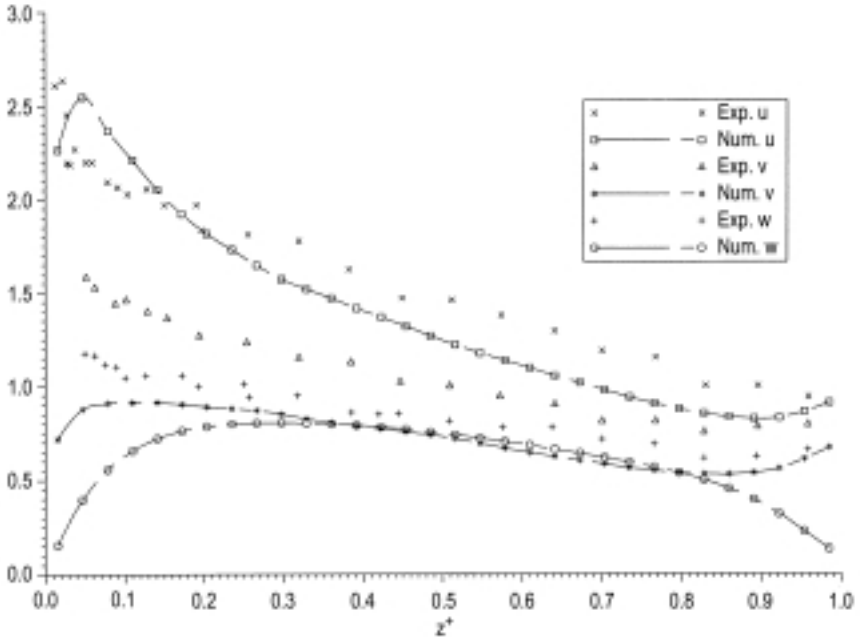

Figure 13.
Comparison of rms between computational solutions and experimental results for box size $6 \times 4 \times 1$ with $32 \times 32 \times 32$ grid using Schumann's split SGM

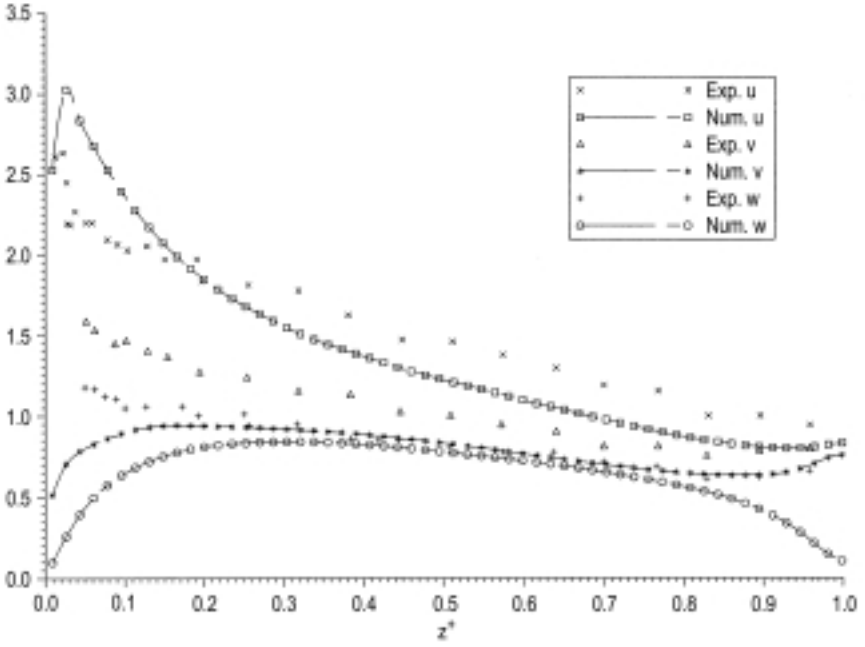

Figure 14.
Comparison of rms between computational solutions and experimental results for box size $6 \times 4 \times 1$ with $64 \times 64 \times 64$ grid using Schumann's split SGM

experimental results. These are shown for the two grids (32^3 and 64^3) used in the last section. It can be seen that the vertical rms agree reasonably well with the measured data. However, greater differences are evident between the numerical and measured streamwise and lateral rms values, particularly near the wall.

8. Conclusions

The use of regular relatively large mesh sizes near wall boundaries has the advantages that less computational points are required and explicit time steps can be larger than would be the case if smaller ones were used. The disadvantages are, however, that the dynamics of the flow in the buffer region are not fully resolved and the simulation can be significantly effected by numerical errors. It is the difficulty in quantifying these errors that prevents any analytical treatment to determine length scales or damping functions. The simulations reported in this paper show that there is no universal valve of C_s which satisfies all of the range of mesh scales, Δ, for the Smagorinsky subgrid model. In this paper, a length scale function based on Mason's matching function but with a varied power is introduced. The simulations show that when a coarse resolution is utilized (i.e. when the streaks near the bed are not sufficiently resolved), then n has to be "tuned" to give reasonable results. A similar situation arises with the use of Schumann's split SGM in which either the mean or turbulent coefficient is set and the other has to be adjusted to reproduce a correct mean velocity profile. For very coarse simulations where the first velocity point occurs well into the buffer region, then only by ensuring that the point falls onto the log-law can accurate mean profiles be obtained. Good LES simulations can, however, be obtained by paying special attention to the lateral resolution and a value $\Delta y^+ < 20$ is suggested.

References

Deardorff, J.W. (1970), "A numerical study of three-dimensional turbulent channel flow at large Reynolds numbers", *J. Fluid Mech*, Vol. 41, pp. 453-80.

Germano, M., Piomell, U., Moin, P. and Cabot, W. (1991), "A dynamic subgrid-scale eddy-viscosity model", *Phs. Fluids A.*, Vol. 3 No. 7, pp. 1760-5.

Ghosal, S., Carati, D. and Moin, P. (1994), *Test of the Dynamic Localization Model on Isotropic Turbulence*, Center for Turbulence Research, Stanford University, Stanford, CA.

Ghosal, S., Lund, T.S. and Moin, P. (1992), *A Dynamic Localization Model for Large-Eddy Simulation of Turbulent Flows*, Center for Turbulence Research, Stanford University, Stanford, CA.

Mason, P.J. and Thomson, D.J. (1992), "Stochastic backscatter in large-eddy simulations of boundary layers", *J. Fluid Mech.*, Vol. 242, pp. 51-78.

Moin, P. and Kim, J. (1982), "Numerical investigation of turbulent channel flow", *J. Fluid Mech.*, Vol. 118, pp. 341-77.

Moin, P., Squires, K., Cabot, W. and Lee, S. (1991), "A dynamic subgrid model for compressible turbulence and scalar transport", *Phys. Fluids A.*, Vol. 3, pp. 2746-57.

Nezu, I. and Rodi, W. (1994), "Open-channel flow measurements with a laser doppler anemometer", *J. Hydraulic Eng., ASCE*, Vol. 112, pp. 335-55.

Schumann, U. (1975), "Subgrid-scale model for finite difference simulations of turbulent flows", *Plane Channels and Annuli, J. Comp. Phys.*, Vol. 18, pp. 376-404.

Smagorinsky, J. (1963), "General circulation experiments with the primitive equations. I. The basic experiment", *Mon. Weather Rev.*, Vol. 91, pp. 99-164.

Thomas, T.G., Leslie, D.C. and Williams, J.J.R. (1995), "Free surface simulations using a conservative 3D code", *J. Comp. Phys.*, Vol. 116, pp. 52-68.

Thomas, T.G. and Williams, J.J.R. (1994), "The numerical simulation of laminar free-surface flows", *J. Hydraulic Res.*, Vol. 32 No. 4.

Thomas, T.G. and Williams, J.J.R. (1995), "Turbulent simulation of open channel flow at low Reynolds number", *Int. J. Heat Mass Transfer.*, Vol. 38 No. 2, pp. 259-66.

Van Driest, E.R. (1956), "On turbulent flow near a wall", *J. Aero. Sci.*, Vol. 23, pp. 1007-11.